Article:
Altaie, A, Bubb, N orcid.org/0000-0002-0010-1253, Franklin, P et al. (3 more authors) (2020) Development and characterisation of dental composites containing anisotropic fluorapatite bundles and rods. Dental Materials, 36 (8). pp. 1071-1085. ISSN 0109-5641

https://doi.org/10.1016/j.dental.2020.05.003

Development and characterisation of dental composites containing anisotropic fluorapatite bundles and rods

Asmaa Altaie[(1)], Nigel Bubb[(2)], Paul Franklin[(1)], Matthew J. German[(3)], Ali Marie[(1)] and David J. Wood[(2)]

a) Division of Restorative Dentistry, School of Dentistry, University of Leeds, UK
b) Division of Oral Biology, School of Dentistry, University of Leeds, UK
c) School of Dental Sciences, Translational and Clinical Research Institute, Faculty of Medical Sciences, Newcastle University, Newcastle upon Tyne, UK

Key Words:

Resin composites; Fluorapatite; strength; Fracture toughness; Fluoride release

Abstract

Objectives

To develop dental composites incorporating fluorapatite (FA) crystals as a secondary filler and to characterise degree of conversion, key mechanical properties and fluoride release.

Methods

FA rod-like crystals and bundles were hydrothermally synthesised and characterised by Scanning Electron Microscopy/ Energy Dispersive X-ray Spectroscopy (SEM/EDS), X-ray Diffraction (XRD) and 19 F MAS-NMR. Composites were formulated containing BisGMA/TEGDMA/BisEMA and barium- aluminium- silicate glass (0FA). FA crystals were incorporated at 10 (10FA), 20 (20FA), 30 (30FA) and 40 wt% (40FA) maintaining a filler content of 80 wt% (63-67 vol%). Degree of conversion (DC), flexural strength (FS), flexural modulus (FM), fracture toughness (K1C), Vickers hardness (HV) and 2-body wear were measured. Fluoride release was measured in neutral and acidic buffers.

Results

XRD and 19 F MAS-NMR confirmed that only FA was formed, whilst SEM revealed the presence of single rods and bundles of nano-rods. DC ranged between 56-60% (>0.05). FA composites showed lower FM and lower FS ($p < 0.05$), but comparable wear resistance and HV ($p > 0.05$) to 0FA. 30FA and 40FA showed similar K1C to 0FA ($p > 0.05$), with SEM showing evidence of toughening mechanisms, whereas 10FA and 20FA showed lower K 1C ($p < 0.05$). FA containing composites released fluoride that was proportional to the amount of FA incorporated ($p < 0.05$) but only under acidic conditions.

Significance

The addition of FA to the experimental composites reduced strength and stiffness but not the DC, hardness or wear rate. 30FA and 40FA had a higher K 1C compared to other FA groups. Fluoride release occurred under an accelerated acidic regime, suggesting potential as a bioactive ‘smart’ composite.

1. Introduction

Resin composites are considered to have superior aesthetics and allow more conservative cavity preparation when compared to amalgam [1–3]. This has led to them becoming increasingly popular for use as direct restorative materials, with around 800 million composite resin restorations placed worldwide in 2015 [4]. Of these restorations approximately 80% were placed in the posterior region, with composite use exceeding amalgam use in several countries [5–8]. With the call for the phase down in the use of mercury containing products, and hence amalgam, due to the Minimata convention, it likely that the use of resin composites will increase worldwide. Current composite formulations have an average life span of just under 10 years after which clinical intervention may be required [9]. Restoration fracture and recurrent caries remain the primary reasons for clinical failures of composite restorations [10–14]. Therefore, it is essential to develop new innovative composite formulations with novel chemistries to enhance their physical and mechanical properties further and that exhibit effective bioactive properties against recurrent caries.

One strategy to enhance the physical properties is by incorporation of hydroxyapatite (HA) particles, rods or whiskers as a filler phase. Given enamel essentially consists of rod-like hydroxyapatite crystals with a high degree of anisotropy, many authors have produced composites containing HA fillers on the basis that the resultant materials would be biocompatible and bioactive [15–20]. These vary from HA whiskers with an aspect ratio > 100 to rods with an aspect ratio of ~5 to particles and materials containing HA as the sole filler or in combination with glass [17,18]. These fillers may be nano- or micro- scale and may be surface treated or silane coupled or not [19,20]. With such a range of experimental parameters and outcomes measured, it is not surprising that the effect of HA reinforcement on many physical properties is somewhat ambiguous.

As well as introducing HA as a filler, a further strategy to produce bioactivity is to introduce bioglass [21] filler particles that are able to release specific ions that will potentially enable the composite to stimulate remineralisation. Bioactive glasses (BAGs) have been used in experimental resin composites [22,23]. BAG has been suggested as a promising bioactive material that can interact with the surrounding environment [24] to precipitate a biologically active hydroxycarbonate layer on their surfaces when they are exposed to bodily fluids. Bioactive glass (BAG) fillers were also reported to increase the fracture toughness of experimental dental composites [25]. Moreover experimental composite materials containing chlorhexidine salts and reactive calcium phosphates as well as glass fillers were developed; materials showed calcium phosphate and chlorhexidine (CHX) release which promoted surface hydroxyapatite/CHX co-precipitation [26]. It was shown that hydroxyapatite precipitation mass was proportional to the CaP content, however the strength of the materials decreased linearly upon raising CaP levels [26].

Finely ground fluorapatite (FA) $Ca_5(PO_4)_3F$ has also been investigated as a potential filler for experimental bioactive dental restoratives [27]. FA is chemically stable but releases fluoride in an acidic environment as the crystals dissolve. Since enamel demineralisation starts when the pH drops below 5.5, FA crystals could be a suitable and effective chemically stable anti-caries material [27] that could mimic the natural caries resistance properties of enamel. A recent study showed that powdered FA crystals (0.6-1µm) could be a potentially suitable filler when incorporated with conventional resin (BisGMA/TEGDMA) forming novel resin composites [28]. It was found that bacterial biofilm mass and colony formation were significantly reduced by the addition of FA to all composites. However using this physical form of FA resulted in a significant reduction in the mechanical properties of the materials.

This study aimed to investigate fillers which could both have an effect on the mechanical properties and have a bioactive role. Whilst BAG fillers do have a potential bioactive function, they tend to be a similar size and isotropic morphology to conventional fillers. Particle anisotropy potentially offers additional toughening mechanisms for fillers in composites that are difficult to obtain simply by size-tuning of spherical particles. Accordingly, the objectives of this study were to develop novel resin composites with micro-, rod like fluorapatite crystals incorporated as a secondary filler and to characterise, as a function of the FA filler content, their degree of conversion, key clinically relevant mechanical properties and fluoride ion release.

2. Materials and Methods

2.1 Fluorapatite (FA) crystal synthesis

Fluorapatite crystals were synthesised using a hydrothermal method [27]. Briefly, 9.36g of ethylenediamine tetra acetic acid calcium disodium salt (EDTA-Ca-Na_2), (Sigma-Aldrich) and 2.07g of $NaH_2PO_4 \cdot H_2O$ (Sigma-Aldrich) were mixed with 90ml of distilled water. The suspension was stirred continuously, and pH adjusted to 6.0 using NaOH. To this solution was added 0.21 g of NaF (Sigma-Aldrich) dissolved in 10 ml water. FA crystal growth was achieved by autoclaving the EDT-Ca-Na_2/NaH_2PO_4/NaF mixture at 121°C at 2.4×10^5 Pa for 10 hours. The powder was then washed five times by adding 100 ml of distilled water and manually stirred for 2 minutes to separate the agglomerates. The powder was then collected and stored in an airtight vial at room temperature.

2.2 Crystal characterisation

Scanning electron microscopy (SEM) coupled with energy dispersive X-ray spectroscopy (EDS) (Hitachi-S-3400N, London, UK) was used to assess the morphology and elemental composition of the powder. XRD analysis (X'pert Philips PW3050, Malvern Panalytical, UK) was performed on the powder from different batches synthesized under identical conditions. Scans were taken between 20-60°, with a step size of 0.05° and dwell of 1 s. The data collected were analysed using

HighScore diffraction software (Malvern Panalytical, UK). Search and match was performed against ICDD 2014 [29]. Following that, crystallography unit cell search and refinements were performed, and crystallographic parameters were calculated [30]. Samples from three different batches of FA was collected, dried and ground to fine powders for solid-state ^{19}F MAS-NMR analysis (600MHz (14.1T) spectrometer (Bruker, Germany). A low fluorine background probe was used to aquire the spectra, in a single-pulse experiment of 30s recycle duration. The ^{19}F chemical shift scale was referenced using the –120 ppm peak of 1M NaF solution, with a secondary reference of $CFCl_3$. Spectra were acquired over a period of 10-24hrs depending on the fluoride level and were an accumulation of between 600 and 1,440 scans.

2.3 Preparation of dental composite formulations

Experimental composites were formulated with monomer:filler ratio of 20:80 wt%. The resin phase was composed of 70%BisGMA:10%TEGDMA:20%BisEMA (ESSTECH Inc, PA, US) to which 1wt% CQ (camphorquinone, Sigma-Aldrich) and 1wt% DMAEMA (dimethylamino ethyl methacrylate, Sigma-Aldrich) were added as photoinitiator and activator and mixed for 60 mins at 60°C using a magnetic stirrer. The primary filler was silanised barium aluminium silicate glass particles (D_{50}=0.7 µm, First Scientific Dental GmbH, Elmshorn, Germany) which was replaced systematically by FA, namely 10 wt% (10FA), 20 wt% (20FA), 30 wt% (30FA) and 40 wt% (40FA), maintaining an overall filler content of 80 wt% (63-66 vol%). A group containing no FA (0FA) was produced as an 80 wt% (67vol %) glass filled control. The resin and filler phases were mechanically mixed for 5 mins at 3000 rpm in a dual asymmetric centrifugal mixer (SpeedMixerTM DAC 150.1 FVZ, Hauschild Engineering and Co. KG, Hamm, Germany). All specimens were stored in lightproof containers at 4°C and tested within 4 weeks of manufacture.

2.4 Degree of Conversion (DC)

Unpolymerised composite was packed manually into the centre of stainless steel washers (diameter = 4mm, thickness= 0.8mm, A2, metric BS4320, RS Components, UK) and then pressed between two glass microscope slides. Representative specimens of each composite were set aside (n=5 per composite) and then the remainder were light-activated polymerised for 5, 10, 20, 30, 40 and 60s respectively. All specimens were exposed to the same light emitting diode (LED) light curing unit (LCU) (Demi Plus, Kerr, Orange Co., CA, USA) at ambient room temperature (23 ± 1ºC) with a spectral range of 450 - 470 nm and an irradiance of 1200 mW/cm^2 (checkMARK Bluelight Analytics Inc., Halifax, Canada).

All DC measurements were made using an ATR-FTIR Spectrometer (Spectrum 100, PerkinElmer, UK) [31–33] between 4000–650 cm^{-1} with 32 co-added scans at 4 cm^{-1} spectral resolution. DC at each time point was determined by calculating the ratio of the absorbance intensities of the aliphatic carbon-carbon (C=C) double bond peak at 1640 cm^{-1} and aromatic carbon-carbon (C=C) double bond peak at 1607 cm^{-1} and comparing it to this same ratio for the uncured material.

2.5 Flexural Strength (FS) and Flexural Modulus (FM)

Flexural modulus and flexural strength were determined following the ISO 4049 [34] using a universal testing machine (Instron 3365, USA) equipped with a three-point bending apparatus. Bar shaped specimens (25 × 2 × 2 mm, n = 10) were prepared using a custom-made split steel mould. The specimens were then stored in distilled water at 37 ± 1ºC for seven days before testing. Prior to testing, specimen thickness and width were measured using digital callipers (±0.01 mm) (Mitutoyo, Japan) and then the specimens were loaded on a 20 mm support span with knife-edge geometry and tested at 0.75 mm/min cross head speed. The maximum load exerted on the specimen at the point of fracture was recorded and flexural modulus (E) and flexural strength were calculated using Equation 1 and Equation 2 respectively.

Equation 1

$$E(GPa) = \frac{l^3 * \delta}{4 * b * h^3 * 1000}$$

Equation 2

$$\sigma\ (MPa) = \frac{3Fl}{2bh^2}$$

where (F) is the maximum load (N) exerted on the specimen, (l) is the distance (mm) between the supports, (b) is the width (mm) at the centre of the specimen, (h) is the height (mm) at the centre of the specimen and (δ) is the slope of a force/deformation curve in the elastic region (N/mm).

2.6 Fracture Toughness (K_{1C})

The sharp single edge notch beam (SENB) method was used to determine the materials' fracture toughness (K_{1C}) following the ASTM (E399-83) standards [35–39]. Bar shaped composite specimens (25 x 6 x 3 mm, n = 10) were made according to ISO 4049 using a custom-made PMMA split mould. After light activated polymerisation, specimens were removed from the mould and a sharp notch (3.0±0.1 mm length x 0.3±0.1 mm width) was cut into each specimen using a custom-made jig containing a diamond disc mounted on a dental hand piece, so that a 2.8±0.1 mm long notch was cut in the centre of the sample. Next, a razor blade mounted on a custom made jig was then passed through the notch to create a very sharp notch (0.2±0.01 mm length). Specimens were polished using P400 silicon carbide abrasive papers (Struers, Denmark) and stored in distilled water at 37 ± 1ºC for seven days prior to testing.

The notched composite specimens were tested in a three-point bending test with a crosshead speed of 0.5 mm/min in a universal testing machine (Instron 3365, USA). Calculations of the fracture toughness values were determined using the following equations:

Equation 3

$$K_{1c} = \left(\frac{3PSa^{1/2}}{2tw^2}\right) \times f\left(\frac{a}{w}\right)$$

Where

Equation 4

$$f\left(\frac{a}{w}\right) = 1.93 - 3.07\left(\frac{a}{w}\right) + 14.53\left(\frac{a}{w}\right)^2 - 25.11\left(\frac{a}{w}\right)^3 + 25.80\left(\frac{a}{w}\right)^4$$

Whereby (P) is the maximum load (N) exerted on the specimen, (S) is the distance (mm) between the supports, (w) is the width (mm) at the centre of the specimen and (t) is the thickness (mm) at the centre of the specimen.

2.7 Vickers Hardness (HV)

Disc shaped composite specimens (6 × 2 mm, n = 5 per composite) were prepared using a custom made steel mould. Specimens were prepared following the ISO 4049 using the same technique reported previously. Composites were then photo-polymerised in one cycle for 40 s and polished using 400 grit silicon carbide abrasive papers (Struers, Copenhagen, Denmark). The specimens were then stored in distilled water in an incubator maintained at 37 ± 1ºC for seven days before testing. All micro-hardness measurements were carried out at an applied load of 100g for 15 s with a diamond pyramidal indentor (Duramin 5, Struers, Denmark). A series of five measurements were recorded for each specimen and mean value was then recorded.

2.8 In-vitro wear testing

Rectangular bar-shaped specimens (20 x 10 x 3mm ±0.1, n=10 per group) were produced using a custom made PMMA holder. Composite was placed into the mould, covered with a cellulose acetate strip and a glass microscope slide and a weight of 1 kg was applied for 20 s to ensure consistent and reproducible packing of the specimens. Next, the entire length of each specimen was light irradiated according to the protocol described in ISO 4049 using the same LCU described previously.

Wear testing was conducted using a pin-on-plate wear testing apparatus originally developed by Harrison and colleagues [40,41]. 8 mm diameter steatite spheres fixed to vertically moving pins were used as the abrading antagonist under a loading force of 4.5 N [40] in a neutral buffer solution (pH 7) to approximate the *in vivo* oral environment [42]. Composite specimens were confined within a PMMA template attached to a horizontal plate moving at a frequency of 2.14 Hz for 4000 cycles the equivalent of three months simulation in the oral cavity [40].

Wear tracks were scanned using a TalySurf CLI 2000 profilometer (Taylor-Hobson Precision, England) equipped with a with a 300 µm range chromatic length aberration (CLA) gauge scanning at 2 mm/s. Longitudinal traces were taken at 4 µm intervals (x-direction) across the wear facet with a measurement recorded at every 40 µm interval (y-direction) thereby generating three dimensional (3D) profile.

2.9 Fluoride Ion release

Disc shaped composite specimens were prepared for each group with dimensions of 6 × 2 mm using a custom made steel mould (n=6). Specimens were prepared following the ISO 4049 standards. Composites were then photo-polymerised in one cycle for 40 s. Composites were then polished using 400 grit silicon carbide abrasive papers (Struers, Denmark) and immersed in 5 ml of pH 4 or pH 7 buffer solutions. The solutions were changed in each container on daily basis in the first week, then every 7 days up to 1 month and then monthly thereafter. The ion-selective method was used to measure the fluoride ion release using an ion-selective electrode (Orion Research, Thermo Scientific, USA) [32,43,44]. Fluoride measurements were taken over 24 hours on daily basis for 7 days, then weekly up to 28 days, then at day 56, 112 and 196. Following fluoride release, specimen surfaces were evaluated using SEM.

2.10 Statistical Analysis

Statistical analysis was conducted using IBM SPSS 21 and Minitab (v18.1, Minitab Inc.). All data sets were assessed for normality using the Kolmogorov– Smirnov test and Shapiro–Wilk test. Data were then analysed using either one-way ANOVA or one-way ANCOVA with post poc Tukey test, or Kruskal–Wallis test with post hoc Bonferroni with a significance level of $p<0.05$ based on their normality.

3. Results

3.1 FA characterisation

SEM analysis of the synthesised FA showed individual hexagonal rod like crystals and bundles, Figure 1. EDS analysis showed that the crystals were calcium rich having a calcium: phosphate ratio of 1.77: 1 and a calcium: fluoride ratio of 4.46: 1.

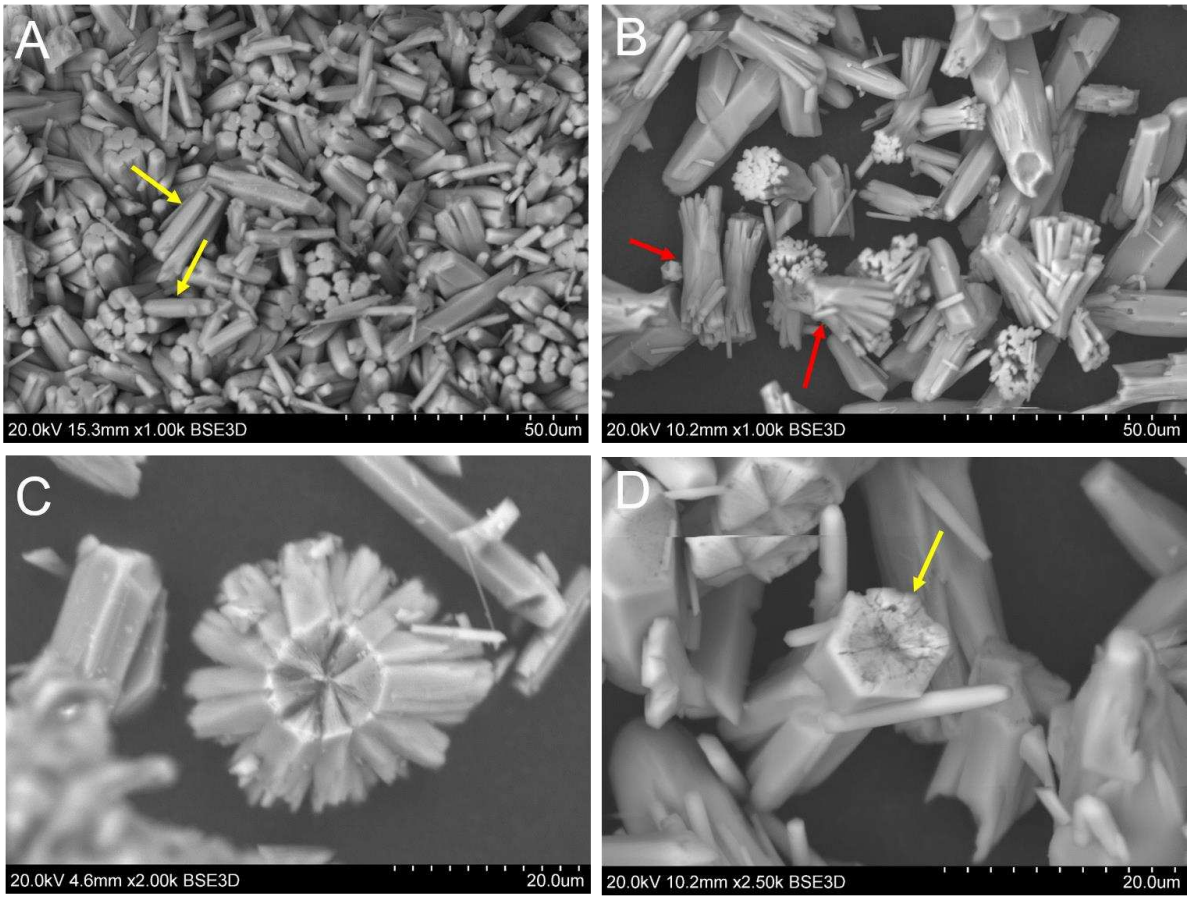

Figure 1: SEM images of the synthesised FA crystals. (A) Shows hexagonally shaped rod like crystals. (B) Shows bundles of FA rods (red arrows) and individual FA rods. (C) Shows as individual bundle with hexagonally shaped centre. (D) Shows an individual hexagonally shaped FA crystal.

A representative powder XRD pattern (Figure 2) displayed narrow peaks indicative of a highly crystalline material, having peak positions corresponding to the reference ICDD FA trace (ref. PDF: 01-079-1572) ICDD 2014. After crystallography analysis diffraction peaks readily indexed to pure hexagonal phase with lattice parameters of a=9.3975 Å, c=6.891 Å and volume=527.01Å3.

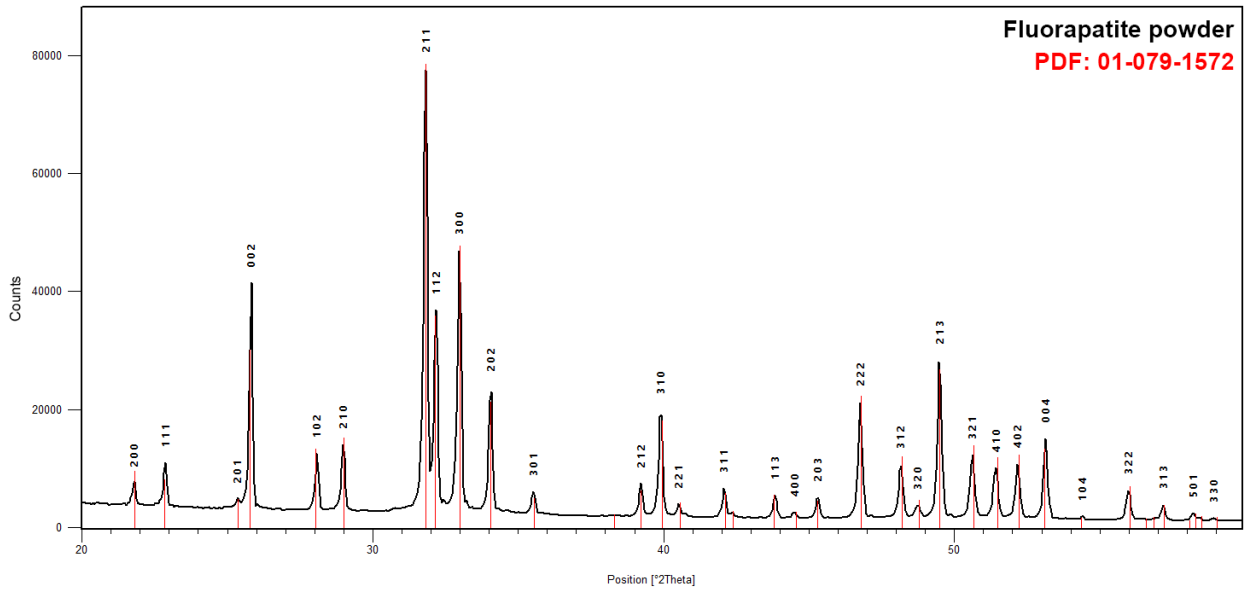

Figure 2: XRD traces of synthesized FA compared to a reference pattern of stoichiometric FA obtained from the International Centre for Diffraction Data (ICDD).

Figure 3 depicts ^{19}F MAS-NMR spectra of synthesised FA, obtained from three different batches synthesised under same conditions. All spectra showed one characteristic peak at –103.6 ppm, indicating that only FA had been produced.

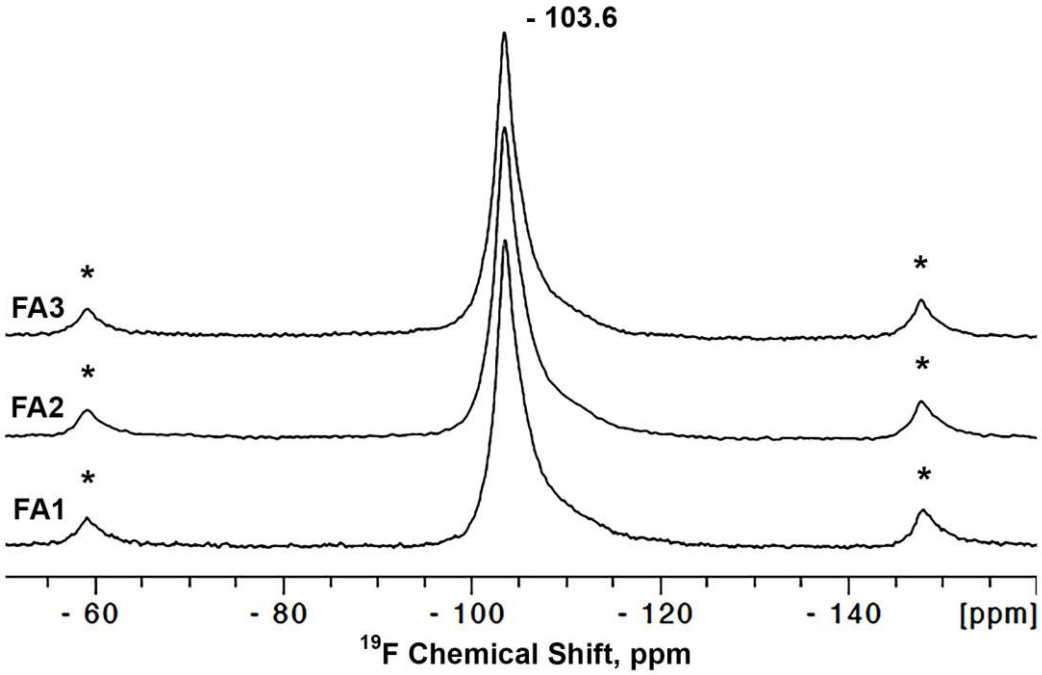

Figure 3: 19F MAS-NMR spectra of FA samples from three different batches FA1, FA2, FA3 synthesised under the same conditions. Asterisks mark spinning side bands.

3.2 Degree of conversion

At very short curing times (5-20 s), there was no consistent relationship between FA content and DC for the model composites, Table 1. After 20s of curing all materials showed greater DC with lower variability between specimens. By 60s of curing there were no significant differences between any of the composites (p>0.05) with a DC of at least 55% found for all materials.

Table 1: The mean degree of conversion and the standard deviation (SD) for FA composites.

Time	0FA		10FA		20FA		30FA		40FA	
	Mean	(SD)	Mean	(SD)	Mean	(SD)	Mean	(SD)	Mean	(SD)
5 s	53.9	(1.8)	53.5	(1.5)	46.4	(2.6)	51.6	(2.2)	45.1	(2.9)
10 s	58.0	(4.2)	50.6	(2.3)	53.2	(0.5)	50.9	(4.7)	45.3	(3.7)
20 s	56.5	(4.1)	56.9	(1.7)	54.8	(4.2)	56.2	(2.0)	50.9	(2.4)
30 s	58.1	(3.9)	53.7	(5.5)	53.0	(6.3)	54.6	(4.7)	50.7	(1.9)
40 s	61.0	(4.6)	57.8	(1.8)	54.8	(7.2)	54.0	(5.4)	56.6	(4.4)
50 s	62.1	(5.1)	59.1	(3.4)	54.8	(7.2)	61.5	(2.8)	53.3	(4.1)
60 s	62.9	(3.6)	56.1	(4.8)	59.8	(4.0)	60.4	(4.4)	55.9	(3.9)

3.3 Physical Properties

As shown in Table 2, the 0FA specimens had the highest flexural strength and modulus of all tested groups ($p<0.05$). As the FA concentration increased there was a sharp decrease in flexural strength and modulus, although this was not statistically significant ($p>0.05$) between the different FA containing groups.

Table 2: Summary of physical properties; flexural strength and modulus, fracture toughness, Vickers hardness and in-vitro wear data (mean, standard deviation).

Group	Flexural Strength (MPa)	Flexural Modulus (GPa)	Fracture toughness ($MPa.m^{1/2}$)	Vickers Hardness (VHN)	Wear Volume (mm^3)
0FA	113.1 (30.1)	14.6 (1.27)	1.3 (0.2)	93.2 (2.8)	0.019 (0.004)
10FA	80.2 (15.8)	12.1 (1.89)	0.9 (0.1)	95.2 (1.6)	0.027 (0.005)
20FA	80.6 (10.0)	12.2 (0.92)	0.9 (0.1)	94.7 (1.7)	0.026 (0.005)
30FA	74.5 (12.5)	12.1 (1.73)	1.5 (0.4)	93.9 (2.3)	0.028 (0.008)
40FA	68.4 (9.4)	12.1 (0.01)	1.2 (0.1)	94.3 (1.9)	0.026 (0.009)

The 10FA and 20FA specimens had significantly lower fracture toughness, compared to the 0FA, 30FA and 40FA specimens ($p<0.05$). SEM analysis of the fractured specimens showed clear cracks extending from the pre-inserted notch with distinctive cleanly fractured surfaces in 0FA composites. However, FA containing composites showed clear cracks with FA bundles and rods bridging the two fractured surfaces, as shown in Figure 4. This was particularly noticeable in the higher wt% FA samples as the crack tip was more likely to engage with a crystal bundle.

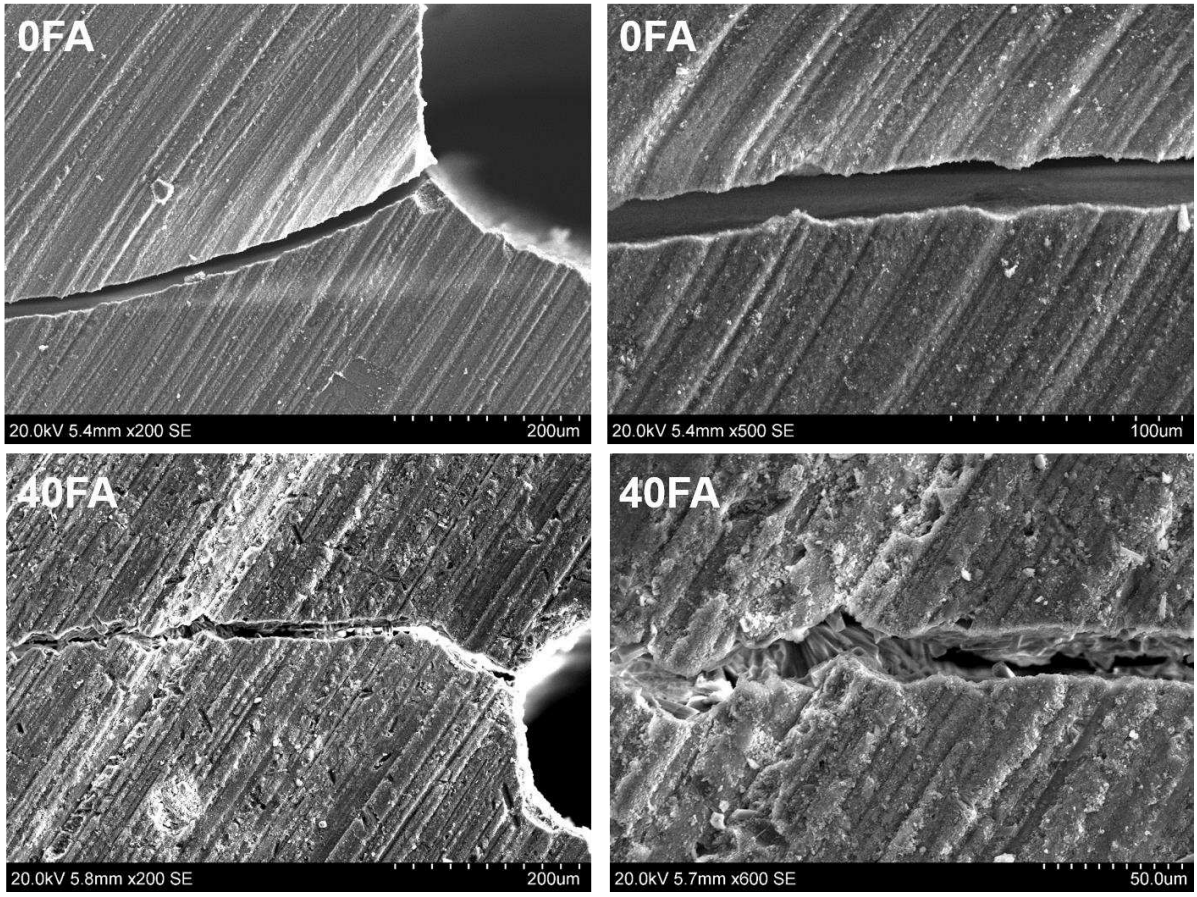

Figure 4: SEM images showing the crack extension from the pre-cracked area and magnifications of the crack line within the samples. 0FA show clear cut crack running through the sample. 40FA shows FA crystals and bundles bridging between the two fractured surfaces.

Fractured specimens showed three distinct zones: (1) The pre-cracked area shows a flat compact surface with the filler particles tightly embedded within the resin matrix, (2) the transitional zone with an irregular surface and displaced filler/matrix and (3) the fractured surface with visible crack lines and detached fillers leaving spaces within the resin matrix, Figure 5.

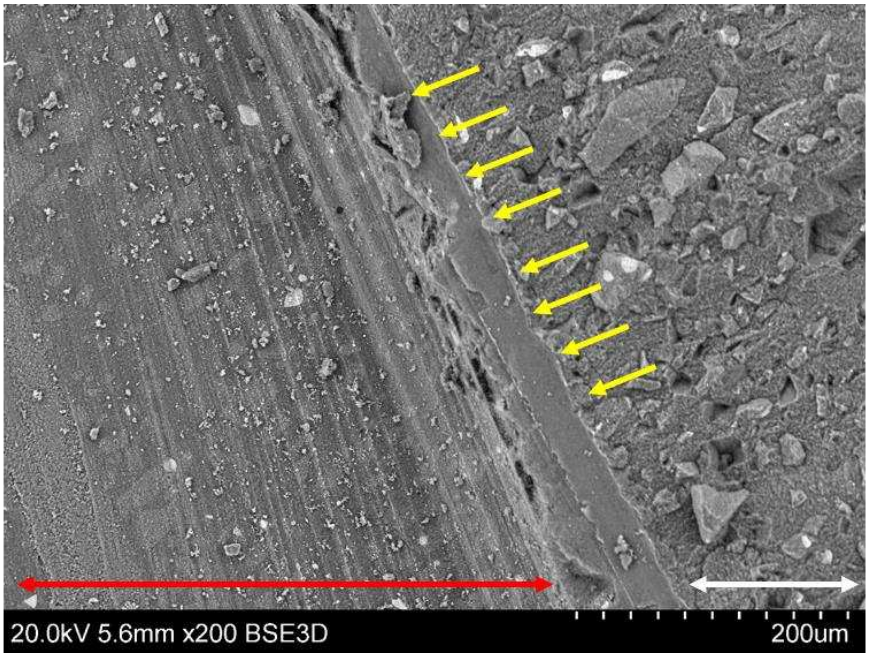

Figure 5: SEM images of 10FA fractured composite specimen showing three fracture zones within the specimen, the pre -cracked surface (red arrow), the transitional zone (yellow arrows) and the fractured surface (white arrow).

Two distinct fracture phenomena were observed: (1) The presence of major and micro crack lines running through the matrix and (2) The detachment of fillers from the resin matrix leaving spaces corresponding to their shape. However, 30FA and 40FA composites specimens also showed distinctive fracture toughening phenomena such as crack deflection and crack bridging near the tip of crack extension. These features were present when the tip of the crack encounters large FA crystals or bundles of crystals, examples shown in Figure 6.

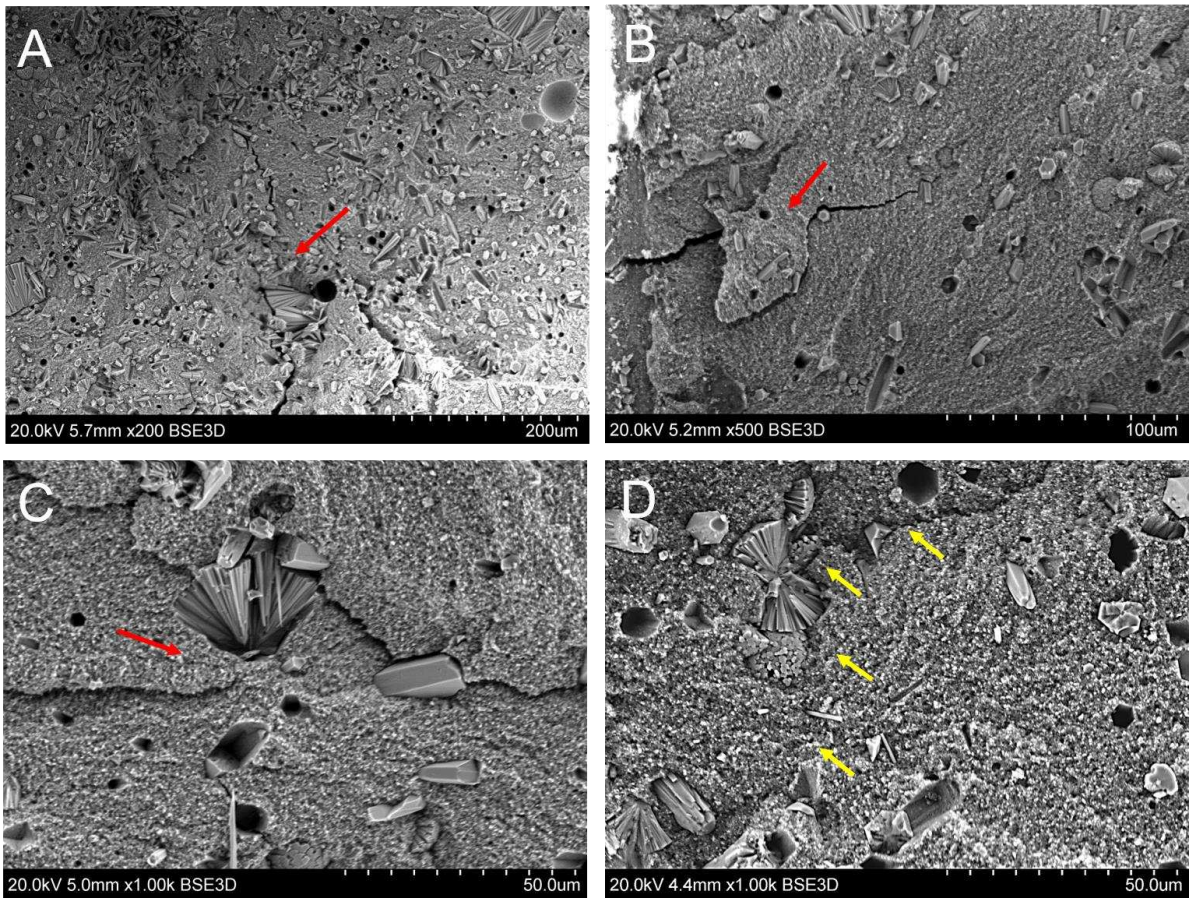

Figure 6: SEM of fracture surfaces of 30FA and 40FA fractured specimens showing typical fracture toughening mechanisms. (A-C) Show crack deflection and crack bridging (red arrows) when FA bundles are encountered and (D) Shows clear crack deflection when encountering an FA bundle which was broken through the middle (yellow arrows).

There were no significant differences found between the hardness of any of the experimental composites (p>0.05), Table 2. All FA containing composites showed similar levels of wear volume (p>0.05), with the 0FA showing the lowest amount of volume loss, although this was not significantly different. SEM analysis of the wear tracks of FA containing composites also showed micro grooves within the resin matrix running in the direction of the wear track; damaged and pulled out individual FA crystals were also seen leaving hexagonal voids within the resin matrix. However, larger FA bundles remained imbedded with the resin matrix with evidence of the assemblies of bundles of FA crystals wearing at the same rate as the rest of the composite, Figure 7. Analysis of the abrading antagonist show round shaped wear facets corresponding to the shape of the wear tracks. EDX analysis of the antagonist wear facet showed Ca and P elements (corresponding to FA) deposited on the surface from the resin composite indicating an adhesive wear mechanism, Figure 8.

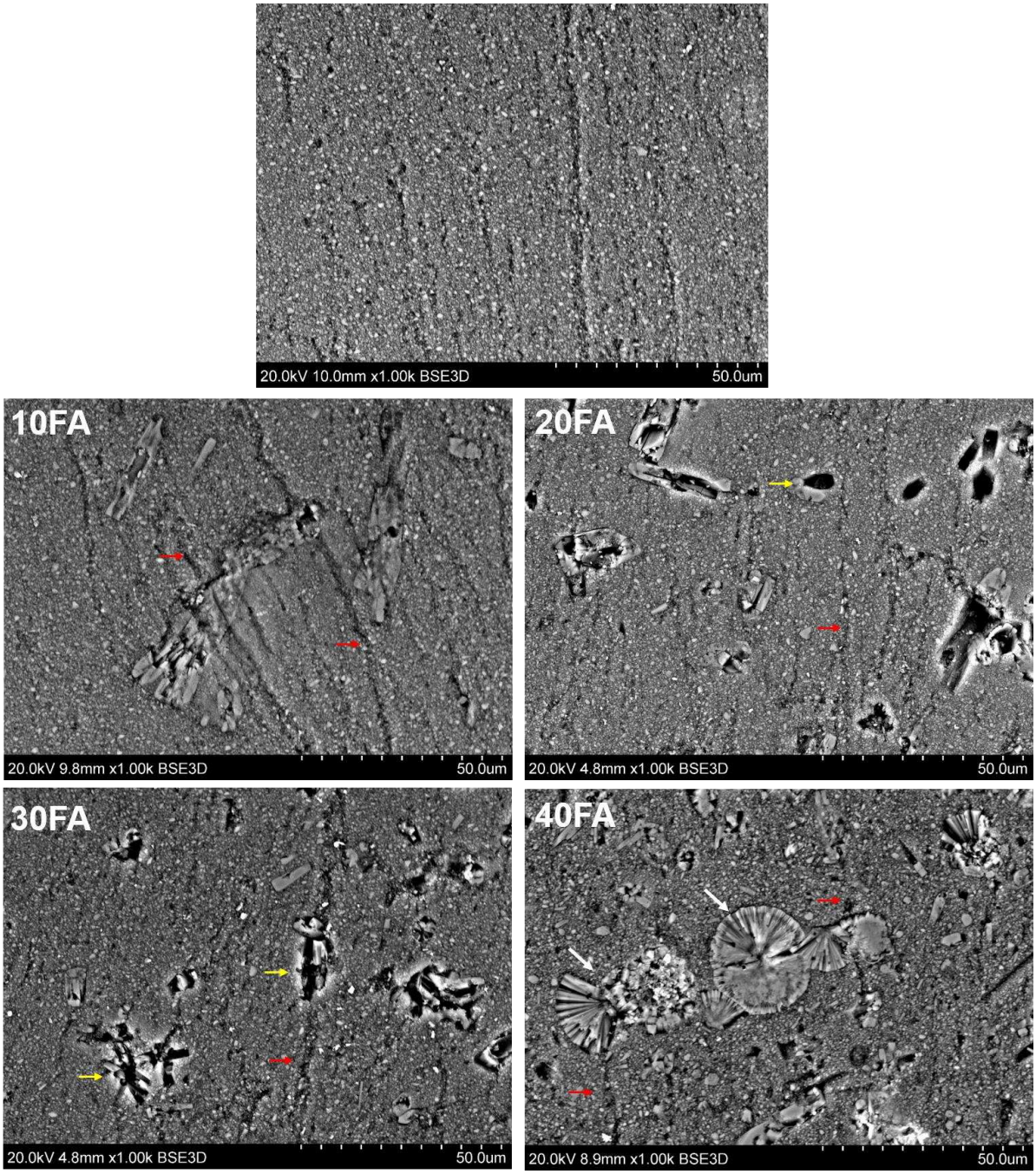

Figure 7: SEM images within the wear tracks of the experimental composites. Typical wear track showed vertical micro grooves running through the matrix (red arrows) and pull out and damage to the FA crystals (yellow arrows). Larger FA bundles were still imbedded within the resin matrix (white arrows).

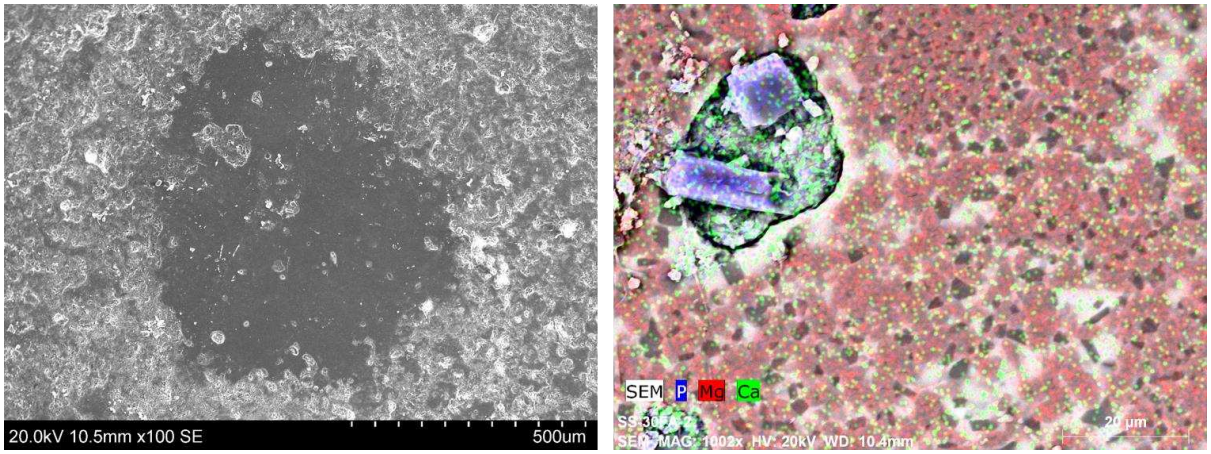

Figure 8: Antagonist surface analysis showing adhesive wear mechanism. (A) SEM image of steatite abrading antagonists corresponding to a wear track of 30FA composite specimen showing evidence of material deposition on the antagonist. FA crystals were shown to be part of this material deposition in the hybrid SEM/elemental mapping image (B). Elemental mapping of the surface confirmed the presence of Ca and which are present in FA but not in the steatite.

3.4 Fluoride ion release

Under neutral conditions, the measured fluoride ions from all FA composites and the control groups were below the electrode threshold value (0.03 µg/cm^2). However under acidic conditions, all FA composites showed detectable fluoride ion release (> 0.03 µg/cm^2), therefore detailed descriptive and statistical analyses were conducted. Initial FA concentration and duration of storage significantly affected fluoride release (p<0.001 for both, one-way ANCOVA). All FA containing composites showed higher cumulative fluoride release over the entire testing period when compared to 0FA, with those containing 20wt%FA or greater exhibiting significantly higher fluoride release (p<0.05).

The pattern of fluoride release was similar amongst all FA containing composites with initial high release on Day 1 followed by a rapid decrease in the amount up to Day 7, Figure 9. 10FA composites continued to release small amounts of fluoride at a consistent rate, but at rates significantly lower than the other FA composites. Post-hoc analysis revealed that the 40FA composites released significantly more fluoride than all other materials over the test period.

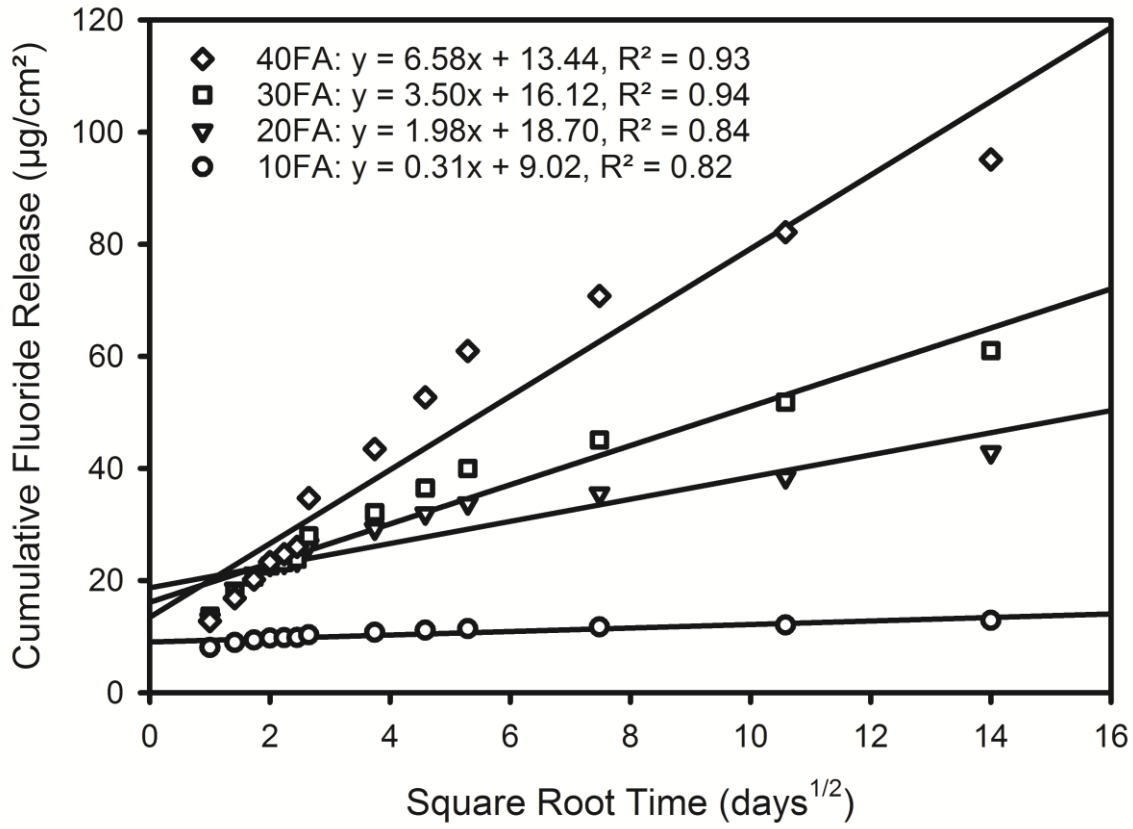

Figure 9: Cumulative fluoride release (µg/cm2) against the square root time (day1/2) of FA composites in pH 4 medium.

Regarding the cumulative fluoride release in relation to the amount of FA used, 20FA, 30FA and 40FA showed significantly higher values when compared to 10FA over the entire tested period ($p<0.05$). However there were no significant differences between 20FA, 30FA and 40 FA in the initial testing period up to Day 7, ($p>0.05$). Significant differences are however evident over extended period of times, 40FA showed higher release compared to 20FA and 30 FA at Day 14 and Day 21 ($p<0.05$). From Day 28 up to Day 196 there were significant differences between all FA containing groups with 40FA showing the highest release (40FA> 30FA > 20FA > 10FA), ($p<0.05$).

Analysis of the fluoride releasing specimens after immersion in pH 4 buffer solution showed evident dissolution of the FA crystals. Figure 10 show representative examples of FA crystals in the 20FA composite before and after immersion in the acidic medium. Initial dissolution of the FA crystals is visible within 24 hours, which then become more evident by Day 28. Most of the FA crystals deposited on the surface showed complete dissolution by Day 112. Elemental mapping of FA composites immersed in acidic medium also showed dissolution of the FA crystals with depletion in the calcium and the phosphate content leaving abundant silica fillers in the resin matrix, Figure 10.

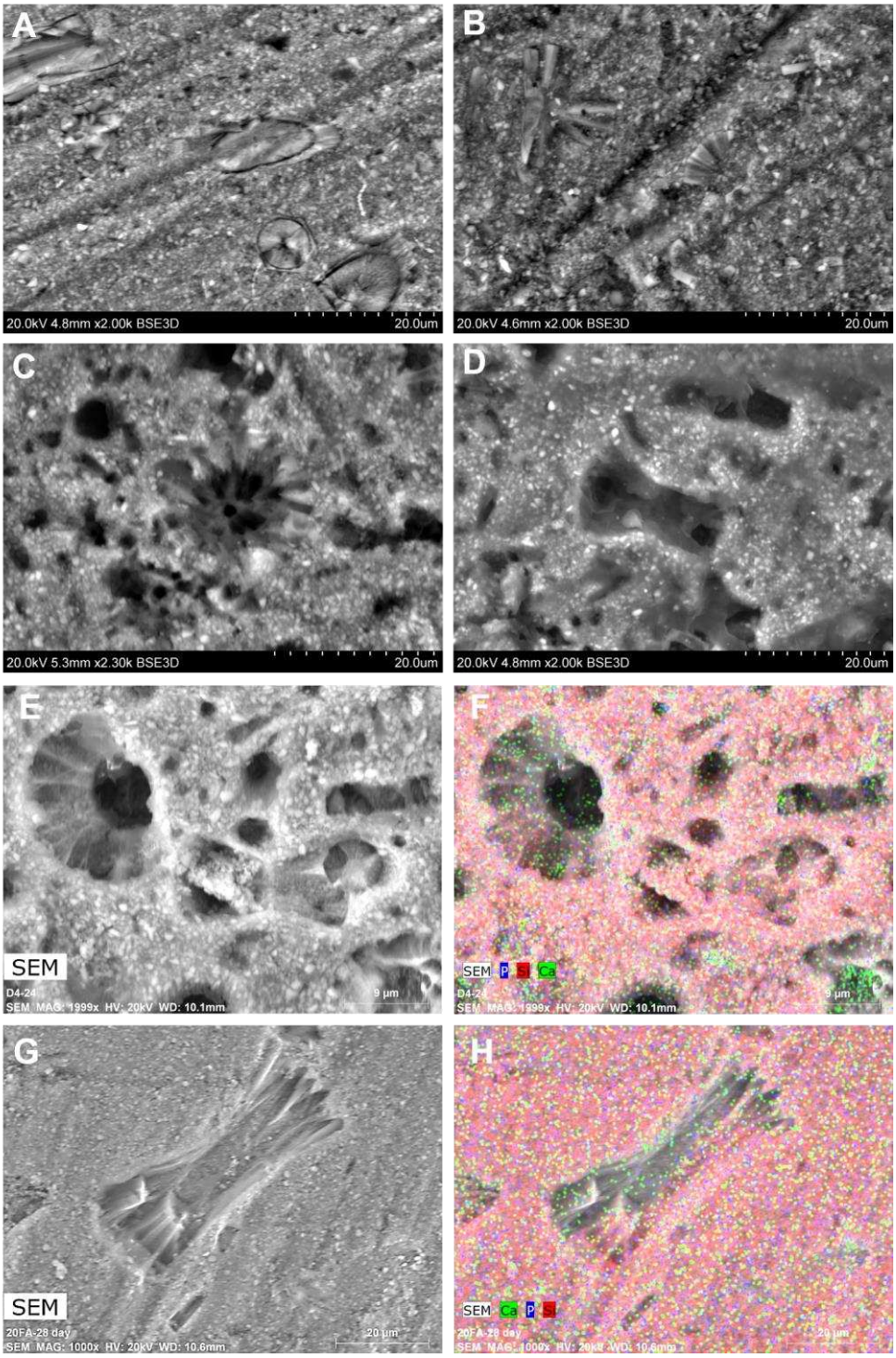

Figure 10: (A-D) SEM images of 20FA composite specimen before and after immersion in pH 4 solution. (A) FA crystals are shown to be embedded within the resin matrix at Day 0, (B) FA crystals starts to dissolve at the top surface within 24 hours of immersion, (C) dissolution continues Day 28 until (D) complete dissolution by Day 112. (E-G) SEM and EDX images with element mapping of 20FA composite specimens after ageing for 28 days in pH 4 buffer solution.

4. Discussion

Hydrothermal synthesis was chosen as the route to produce the anisotropic FA crystals as it is a bottom-up method with high yields and structural purity and by varying key parameters such as pH it is possible to control size, shape, structure, composition and surface chemistry [45].

SEM revealed two distinct crystal morphologies. As shown in Figure 1 (A and D), well-defined, thermodynamically stable, rod-like FA [$Ca_{10}(PO_4)_6F_2$] crystals with a typical apatite hexagonal structure and a long c axis were created after autoclaving for 10 h; these crystals were between 10-30 μm long with an aspect ratio of between 5-10 to 1. However, SEM also revealed Figure 1 (B and C) 'anisotropic superstructures' [46] consisting of smaller diameter (approx. 1 μm wide) bundles or clusters of FA crystals. These FA structures will have the tendency to aggregate together, side by side, to form a bundle because of the stronger van der Waals attraction along the long axis of the rods than at the rod ends [27]. These bundles were approximately 20 μm long with a smaller aspect ratio of 3-4 to 1.

XRD and ^{19}F MAS-NMR confirmed that the synthesised powder consisted only of fluorapatite. The XRD traces displayed narrow peaks indicative of a highly crystalline material, having peak positions corresponding to the reference ICDD FA trace as shown in Figure 2. ^{19}F MAS-NMR spectra also indicated that fluorapatite was the only chemical species formed, Figure 3; spectra showed the characteristic peak at -103.6 ppm corresponding to the F-Ca(3) triangles in the apatite structure. Therefore, based on previous reported findings by Gao et al. this indicates 100% substitution of OH^- with F^- suggestion pure FA formation [47]. This is also in agreement with Clarkson et al. showing similar spectra of FA [48].

Experimental dental composites were successfully produced with FA incorporated at 10-40%wt while maintaining overall filler content of 80%wt (63-67%vol). The clinical performance of dental composites has been related to a number of mechanical properties [49,50]; consequently, the materials were subjected to a rigorous series of tests to characterise their properties with the aim of establishing whether the experimental composites were potentially suitable for use as an occlusal filling material.

The addition of FA did not affect the degree of conversion of the experimental materials regardless of the amount of FA incorporated. The degree of conversion of FA composites ranged between 50 and 61% at curing times greater than 20 s and up to 60 s, similar to the DC found for most commercial resin composites [51]. At shorter curing times (5-10 s) FA composites with highest concentration of FA (40%) showed significantly lower DC compared to 0FA and 10FA. The polymerisation process is affected by several factors including the material's composition, photoinitiator chemistry, curing protocol, specimen geometry, surrounding temperature and the presence of oxygen. Light transmission through the material is a key factor in determining the extent of polymerisation. Insufficient light transmission

is associated with surface reflection [31,52], scattering effect of the filler particles [53], absorption [54] and the interfacial resin/filler refraction [55]. As the refractive index of the resin approaches that of the filler, the scattering at the interfacial filler/resin reduces which results in higher light transmission. Therefore, a mismatch between the refractive indices of the filler/resin could result in a reduction in light transmission and consequently lower maximum rates of polymerisation [55,56]. The refractive index of FA is around 1.63, whereas barium glass is around 1.53, and BisGMA: TEGDMA (70:30%) index is around 1.52 [55]. Therefore, the lower DC of 40FA composites could be attributed to the higher FA content leading to possible reduction in the light transmission as a consequence of scattering at the resin/FA interface. However, the DC at extended curing times (20-60 s) showed no significant differences between all the FA containing groups regardless of the FA concentration used. It should be noted that ATR-FTIR only analyses the material close to the surface due to the limited penetration of the laser in this mode. Consequently, due to the potential scattering effect of the FA filler there may be lower levels of conversion at deeper sections within the restoration. Future work should, therefore, include an evaluation of the DC at deeper levels within the composite specimen.

The properties for evaluating resin composites measured in this study (i.e. 3-point bending strength, flexural modulus, fracture toughness, indentation hardness and two-body wear) are five of the seven ranked first in the priority of measurements as recommended in the Academy of Dental Materials recent guidance [57] of tests which were useful, applicable, supported by the literature and show a correlation with clinical findings. This study therefore comprehensively evaluates the mechanical properties of these novel resin based composites and does so with a wider range of tests than have previously been used with apatite reinforced composites.

In the present study, whilst there was a decrease in flexural strength as the FA concentration increased, there was no significant difference found between any of FA groups; the FA-free specimens (0FA) had the highest flexural strength but also a relatively high standard deviation. In terms of stiffness, the 0FA specimens had the highest flexural modulus. Zhang and Zhang [17] reported a reduction in flexural strength for both silane treated and untreated nanoscale rod HA fillers at relatively low filler contents (max 19 vol%) which was attributed to flaws propagating through pores and voids in the HA aggregates. Chen et al [19] reported an increase in biaxial flexural strength in composites containing HA nanofibers with and without treatment but this increase was only seen at low HA addition, and had gone by 10% replacement, below the levels used in the current study and even these composites only had a maximum filler content of 60 wt%, whereas those in the current study had 80 wt%. Agglomeration of HA fibres was again postulated as a reason for the loss of mechanical advantage at higher (15%) filler loadings. In the current study we used a dual asymmetric centrifugal mixer specifically designed for making high viscosity, highly filled materials and this has resulted in materials with little evidence of FA agglomeration or porosity as a consequence of material compounding.

Fracture toughness (K_{1C}) has been reported to correlate to clinical fractures of resin composites [50]. Low concentrations of FA (10 and 20 wt%) led to a significant reduction in the fracture toughness compared to the FA-free specimens and higher FA concentrations. SEM analysis of fractured composite specimens showed typical features of failure mechanisms; cracks were initiated from the pre-cracked area, which then continued to extend through the filler/resin interface and detached individual FA crystals protruding on one surface and leaving hexagonal spaces on the opposing surface. However, interesting observations were found in 30FA and 40FA composites where distinctive fracture toughening mechanisms were identified including crack deflection and bridging. These mechanisms often act together in which crack deflection leads to crack bridging [58] similar to natural tooth tissues by which the enamel and dentine are toughened [59–61]. The unique morphology of FA crystals allowed microscopic crack deflection and crack bridging which sustained a portion of the applied load that otherwise would have gone towards crack extension. Therefore, we hypothesise that the increased fracture toughness of 30FA and 40FA could be attributed to the crack interacting with FA crystals/bundles which were more prevalent as FA wt% increased. This study therefore highlights the importance of filler morphology as well as amount of filler in affecting key mechanical properties. Fracture toughness is an intrinsic material property and should be independent of test method. However, this is not the case for dental composites and there are limitations in using the SENB method for measuring fracture toughness, as indeed there are for all fracture toughness testing methods [35]. In particular, for SENB testing, there are issues in introducing a consistent sharp pre-crack into the samples and the effect of slow crack growth in samples prior to testing. The original standards from which this test arises are based on metals and require the pre-crack to be introduced by fatigue. This is not feasible for dental composites and hence authors have used cutting wheels/ blades to introduce a sharp crack into samples for SENB testing. It is important that great care is taken in this stage of sample preparation. The Academy of Dental Materials in their recent guidance [57] recommended the use of the SENB test for fracture toughness measurement, whilst recognising the difficulties inherent in introducing true pre-cracks and the variations between studies that this introduces. A recent study by Alshabib et al. [62] on hydroxyapatite short fibre reinforced dental composites recorded fracture toughness values using SENB of 0.96 – 2.14 $MPa.m^{1/2}$ similar to those recorded in the current study. The authors noted that genuine differences between samples could be seen as specimen preparation and measurement conditions were constant.

0FA specimens generally exhibited high flexural strength, flexural modulus and fracture toughness values. The 0FA specimens contained only silane-coated barium glass particles as the filler phase, meaning that there was likely to be good integration between the matrix and the filler phase in the polymerised composite, a factor that has been previously shown to be necessary for optimum composite mechanical properties [63–65]. FA rods were not silane coated, meaning that only the primary filler phase would interact with the matrix. This lack of coupling on filler

particles can lead to the particles acting like large inclusions, increasing the risk of crack initiation and propagation under applied stress [16,22,25,66]. In future, it would be valuable to investigate the effect of surface coupling of the FA crystals on the mechanical properties of FA composites. However, it is important to realise that silane coating of bioactive fillers can affect the water adsorption and solubility of composites containing them [67], which could potentially reduce the ion release of bioactive composites, so there may be a compromise between optimising mechanical properties and maintaining bioactivity.

FA containing composites showed high microhardness values, comparable to most highly filled commercial composites. The addition of FA had no effect on the microhardness irrespective of the FA concentration. As a direct correlation has been established between the filler content and dental composite microhardness [64,65,68,69] it is likely that the high microhardness values measured here are attributed to their high overall filler content, which was kept constant, rather than the type of filler.

The wear resistance of all FA containing composites was similar to 0FA. All of the FA composites had a filler volume fraction greater than 60vol%, which has been shown to be the minimum threshold value to maintain adequate mechanical strength and wear resistance [70]. However, the wear process remains complex and the mechanism of wear was different between FA containing composites and 0FA. SEM images showed similar patterns of wear across the experimental groups with three dominant features; (1) cracks running through the matrix in the direction of wear, (2) displacement of individual FA rod-like crystals and (3) evidence of the assemblies of bundles of FA crystals wearing at the same rate as the composite. Generally combinations of wear mechanisms were present across all composite groups, however FA composites showed a secondary adhesive wear mechanism where isolated FA crystals were transferred onto the abrading antagonist by cold welding through friction [71,72].

Fluoride has been identified as an effective agent in slowing caries progression through enhancing the remineralisation and reducing the demineralisation of enamel and dentine [73]. Therefore, the idea of fluoride releasing restoratives is very attractive to maintain constant fluoride release in the mouth and in close proximity to demineralising tooth tissue. Under acidic conditions, all FA composites released statistically significant amounts of fluoride when compared to the control groups ($p<0.05$). Under neutral conditions, no fluoride release was detected from the FA composites and the control groups. The amount of fluoride release of restorative materials varies in the literature and is dependent on the type of storage medium [74]. Generally, the highest amount of fluoride release is shown to be in acidic environments [75].

The pattern of fluoride release was similar for the FA composites, being highest in the first day and diminishing subsequently. The fluoride release was proportional to square-root time, with the rate of release increasing proportional to the concentration

of FA in the composite. Despite the fluoride release being proportional to time, at early time points, all the FA composites exhibited a non-linear response, indicating that there was an initial burst-release phase [74]. This pattern is similar to most restorative materials where initial high amounts of fluoride release is detected within 24-48 hours, which rapidly diminishes with time and long term release continues at much lower rates [75,76]. The amount of fluoride released from the FA composites was significantly lower than that released from GICs, for instance an order of magnitude lower than the levels reported by Karantakis et al. [75].

However unlike the currently available fluoride releasing restorative materials such as glass ionomer cements, the developed FA composites showed no release under neutral conditions. Fluorapatite has been reported to be chemically stable but known to release fluoride under acidic conditions. The results of this study showed that FA maintained the same behaviour when added to resin composites. All FA composites released fluoride when they were subjected to pH 4 medium due to the dissolution of FA crystals. Since enamel demineralisation starts when the pH drops below 5.5, FA composites could be a suitable restorative material to minimise demineralisation and progression of recurrent caries around resin composites. Therefore, FA composites could potentially be considered as a "smart" restorative that releases fluoride only when it is required as the pH drops in the oral cavity [77]. To date, there has been no consensus on the amount of fluoride required for a restorative material to be effective against recurrent caries; however it is generally suggested that the effect of fluoride releasing restoratives is mostly due to the localised fluoridation adjacent to the demineralisation zones rather than elevation of fluoride levels in saliva. It has been reported that localised small amounts of fluoride approximately in the ranges of 0.03-0.08 ppm and 0.63-1.3 µg F^-/cm^2/day is sufficient to shift the equilibrium from demineralisation to re-mineralisation [74,78]. Therefore all FA composites showed fluoride release within the range considered to be effective in preventing demineralisation. In addition to that, the amount of fluoride is considerably higher when compared to the commercially available fluoride releasing dental composite [75,79].

It was evident from the SEM images that the mechanism by which fluoride was released from the FA composites was due to the dissolution of the FA crystals when subjected to acidic environment. The initial high daily release followed by a reduced but sustained release may simply be due to the fact that at extended time points, there was little FA remaining. SEM showed that the FA rods could be completely dissolved at these time points, leaving holes where crystals had been once; it is acknowledged that this may impact on the mechanical properties of the materials. However it is important to note that this was a vastly accelerated degradation study and that a patient's exposure to acid in the oral cavity is infrequent and episodic in nature and that saliva effectively buffers the acid challenges a patient experiences due to eating/drinking [33]. Nevertheless, it would be worth evaluating the mechanical properties of these materials following fluoride ion release and in using pH cycling models to mimic the demineralisation and remineralisation processes.

This may provide further insight into the behaviour of FA composites which might be a suitable “smart” composite that react with the surrounding environment and may prevent recurrent caries progression. Surface coupling may further enhance the mechanical properties of FA composites; conversely the fluoride releasing properties may be affected. Therefore, further research is suggested to investigate the possibility of surface coupling of FA followed by re-evaluation of the materials properties.

In summary, this study suggests an alternative approach to introduce bioactive properties to resin composites by incorporating synthesised fluorapatite as secondary filler. Novel fluorapatite containing resin composites were successfully produced which exhibited adequate key physical and mechanical properties. Additionally these novel formulations have the advantage of short and long term fluoride ion release.

5. Conclusions

Highly filled experimental composites were successfully produced incorporating FA as secondary filler; the addition of FA affected key physical and mechanical properties. The unique morphology of FA crystals enhanced fracture toughening mechanisms in FA containing composites leading to increased fracture toughness when higher concentrations of FA were used. FA containing composites showed short and long term fluoride release under acidic conditions showing a promising step towards a potential “smart” fluoride releasing dental composite.

Funding

This research did not receive any specific grant from funding agencies in the public, commercial, or not-for-profit sectors

Acknowledgments

The authors would like to acknowledge Professor Robert Hill at the Institute of Dentistry, Dental Physical Sciences, Queen Mary University of London for his assistance in the ^{19}F MAS-NMR.

References

[1] Beazoglou T, Eklund S, Heffley D, Meiers J, Brown LJ, Bailit H. Economic impact of regulating the use of amalgam restorations. Public Heal Rep 2007;122:657–63.

[2] Lynch CD, Shortall AC, Stewardson D, Tomson PL, Burke FJ. Teaching posterior composite resin restorations in the United Kingdom and Ireland: consensus views of teachers. Br Dent J 2007;203:183–7.

[3] Lynch CD, Frazier KB, McConnell RJ, Blum IR, Wilson NH. Minimally invasive management of dental caries: contemporary teaching of posterior resin-based composite placement in U.S. and Canadian dental schools. J Am Dent Assoc 2011;142:612–20.

[4] Jäggi F. Filling materials—quantity reports. Corporate MarketInsight, Ivoclar Vivadent. 2015.

[5] Burke FJT. Amalgam to tooth-coloured materials - implications for clinical practice and dental education: governmental restrictions and amalgam-usage survey results. J Dent 2004;32:343–50.

[6] Mitchell RJ, Koike M, Okabe T. Posterior amalgam restorations—usage, regulation, and longevity. Dent Clin North Am 2007;51:573–89.

[7] Vidnes-Kopperud S, Tveit AB, Gaarden T, Sandvik L, Espelid I. Factors influencing dentists' choice of amalgam and tooth-colored restorative materials for Class II preparations in younger patients. Acta Odontol Scand 2009;67:74–9.

[8] Burke FJT, Wilson N, Creanor S, Brunton P. Materials used by UK dentists: Results of a Questionare. IADR 2017.

[9] Ástvaldsdóttir Á, Dagerhamn J, van Dijken JW V, Naimi-Akbar A, Sandborgh-Englund G, Tranæus S, et al. Longevity of posterior resin composite restorations in adults–a systematic review. J Dent 2015;43:934–54.

[10] Soncini JA, Maserejian NN, Trachtenberg F, Tavares M, Hayes C. The longevity of amalgam versus compomer/composite restorations in posterior primary and permanent teeth: findings From the New England Children's Amalgam Trial. J Am Dent Assoc 2007;138:763–72.

[11] Bernardo M, Luis H, Martin MD, Leroux BG, Rue T, Leitao J, et al. Survival and reasons for failure of amalgam versus composite posterior restorations placed in a randomized clinical trial. J Am Dent Assoc 2007;138:775–83.

[12] Sunnegardh-Gronberg K, van Dijken JW, Funegard U, Lindberg A, Nilsson M. Selection of dental materials and longevity of replaced restorations in Public Dental Health clinics in northern Sweden. J Dent 2009;37:673–8.

[13] Demarco FF, Correa MB, Cenci MS, Moraes RR, Opdam NJM. Longevity of posterior composite restorations: Not only a matter of materials. Dent Mater 2012;28:87–101.

[14] Beck F, Lettner S, Graf A, Bitriol B, Dumitrescu N, Bauer P, et al. Survival of direct resin restorations in posterior teeth within a 19-year period (1996-2015): A meta-analysis of prospective studies. Dent Mater 2015;31:958–85.

[15] Arcís RW, López-Macipe A, Toledano M, Osorio E, Rodríguez-Clemente R, Murtra J, et al. Mechanical properties of visible light-cured resins reinforced with hydroxyapatite for dental restoration. Dent Mater 2002;18:49–57.

[16] Taheri MM, Abdul Kadir MR, Shokuhfar T, Hamlekhan A, Shirdar MR, Naghizadeh F. Fluoridated hydroxyapatite nanorods as novel fillers for improving mechanical properties of dental composite: Synthesis and application. Mater Des 2015;82:119–25.

[17] Zhang H, Zhang M. Effect of surface treatment of hydroxyapatite whiskers on the mechanical properties of bis-GMA-based composites. Biomed Mater 2010;5:054106. https://doi.org/10.1088/1748-6041/5/5/054106.

[18] Chiari MDS, Rodrigues MC, Xavier TA, De Souza EMN, Arana-Chavez VE, Braga RR. Mechanical properties and ion release from bioactive restorative composites containing glass fillers and calcium phosphate nano-structured particles. Dent Mater 2015;31:726–33. https://doi.org/10.1016/j.dental.2015.03.015.

[19] Chen L, Xu C, Wang Y, Shi J, Yu Q, Li H. BisGMA/TEGDMA dental nanocomposites containing glyoxylic acid-modified high-aspect ratio hydroxyapatite nanofibers with enhanced dispersion. Biomed Mater 2012;7:045014. https://doi.org/10.1088/1748-6041/7/4/045014.

[20] Li X, Liu W, Sun L, Aifantis KE, Yu B, Fan Y, et al. Resin composites reinforced by nanoscaled fibers or tubes for dental regeneration. Biomed Res Int 2014:542958. https://doi.org/10.1155/2014/542958.

[21] Davis HB, Gwinner F, Mitchell JC, Ferracane JL. Ion release from, and fluoride recharge of a composite with a fluoride-containing bioactive glass. Dent Mater 2014;30:1187–94.

[22] Alania Y, Chiari MDS, Rodrigues MC, Arana-Chavez VE, Bressiani AHA, Vichi FM, et al. Bioactive composites containing TEGDMA-functionalized calcium phosphate particles: Degree of conversion, fracture strength and ion release evaluation. Dent Mater 2016;32:e374–81.

[23] Hyun H-K, Salehi S, Ferracane JL. Biofilm formation affects surface properties of novel bioactive glass-containing composites. Dent Mater 2015;31:1599–608.

[24] Hench LL. The story of Bioglass. J Mater Sci Mater Med 2006;17:967–78. https://doi.org/10.1007/s10856-006-0432-z.

[25] Khvostenko D, Mitchell JC, Hilton TJ, Ferracane JL, Kruzic JJ. Mechanical performance of novel bioactive glass containing dental restorative composites. Dent Mater 2013;29:1139–48. https://doi.org/10.1016/j.dental.7013.08.707.

[26] Aljabo A, Abou Neel EA, Knowles JC, Young AM. Development of dental composites with reactive fillers that promote precipitation of antibacterial-hydroxyapatite layers. Mater Sci Eng C 2016;60:285–92. https://doi.org/10.1016/j.msec.2015.11.047.

[27] Chen H, Tang Z, Liu J, Sun K, Chang SR, Peters MC, et al. Acellular Synthesis of a Human Enamel-like Microstructure. Adv Mater 2006;18:1846–51. https://doi.org/10.1002/adma.200502401.

[28] Van der Laan HL, Zajdowicz SL, Kuroda K, Bielajew BJ, Davidson TA, Gardinier J, et al. Biological and Mechanical Evaluation of Novel Prototype Dental Composites. J Dent Res 2019;98:91–7. https://doi.org/10.1177/0022034518795673.

[29] ICDD 2014. Powder Diffraction File Inorganic and Organic Data Book, 2014. PDF: 01-079-1572. Edited by Dr. Soorya Kabekkodu. International Centre for Diffraction Data, Newtown Square, PA USA.

[30] Crystallography Open Database COD, 2013 (REV89244, Nov 2013), (COD 9001878), Bruker AXS GmbH, Germany.

[31] Ilie N, Hickel R. Quality of curing in relation to hardness, degree of cure and polymerization depth measured on a nano-hybrid composite. Am J Dent 2007;20:263–8.

[32] Durner J, Obermaier J, Draenert M, Ilie N. Correlation of the degree of conversion with the amount of elutable substances in nano-hybrid dental composites. Dent Mater 2012;28:1146–53. https://doi.org/10.1016/j.dental.2012.08.006.

[33] Walters NJ, Xia W, Salih V, Ashley PF, Young AM. Poly(propylene glycol) and urethane dimethacrylates improve conversion of dental composites and reveal complexity of cytocompatibility testing. Dent Mater 2016;32:264–77. https://doi.org/http://dx.doi.org/10.1016/j.dental.2015.11.017.

[34] ISO 4049 (2009). Polymer-based restorative materials

[35] Fujishima A, Ferracane JL. Comparison of four modes of fracture toughness testing for dental composites. Dent Mater 1996;12:38–43. https://doi.org/10.1016/s0109-5641(96)80062-5.

[36] Bonilla ED, Yashar M, Caputo AA. Fracture toughness of nine flowable resin composites. J Prosthet Dent 2003;89:261–7. https://doi.org/http://dx.doi.org/10.1067/mpr.2003.33.

[37] Musanje L, Ferracane JL. Effects of resin formulation and nanofiller surface treatment on the properties of experimental hybrid resin composite. Biomaterials 2004;25:4065–71. https://doi.org/http://dx.doi.org/10.1016/j.biomaterials.2003.11.003.

[38] Rodrigues Junior SA, Scherrer SS, Ferracane JL, Della Bona A. Microstructural characterization and fracture behavior of a microhybrid and a nanofill composite. Dent Mater 2008;24:1281–8. https://doi.org/10.1016/j.dental.2008.02.006.

[39] Soderholm K-J. Review of the fracture toughness approach. Dent Mater 2010;26:E63–77. https://doi.org/10.1016/j.dental.2009.11.151.

[40] Harrison A, Lewis TT. Development of an abrasion testing machine for dental materials. J Biomed Mater Res 1975;9:341–53. https://doi.org/10.1002/jbm.820090309.

[41] Harrison A, Draughn RA. Abrasive wear, tensile strength, and hardness of dental composite resins--is there a relationship. J Prosthet Dent 1976;36:395–8. https://doi.org/10.1016/0022-3913(76)90160-8.

[42] Antunes PV, Ramalho A. Influence of pH values and aging time on the

tribological behaviour of posterior restorative materials. Wear 2009;267:718–25. https://doi.org/10.1016/j.wear.2008.12.054.

[43] Itota T, Carrick TE, Yoshiyama M, McCabe JF. Fluoride release and recharge in giomer, compomer and resin composite. Dent Mater 2004;20:789–95. https://doi.org/10.1016/j.dental.2003.11.009.

[44] Itota T, Carrick TE, Rusby S, Al-Naimi OT, Yoshiyama M, McCabe JF. Determination of fluoride ions released from resin-based dental materials using ion-selective electrode and ion chromatograph. J Dent 2004;32:117–22.

[45] Earl J, Wood D, Milne S. Dentine infiltration a cure for sensitive teeth. Am Ceram Soc Bull 2006;85:22–5.

[46] Shen J, Jin B, Jiang Q ying, Hu Y min, Wang X yan. Morphology-controlled synthesis of fluorapatite nano/microstructures via surfactant-assisted hydrothermal process. Mater Des 2016;97:204–12. https://doi.org/10.1016/j.matdes.2016.02.091.

[47] Gao Y, Karpukhina N, Law R V. Phase segregation in hydroxyfluorapatite solid solution at high temperatures studied by combined XRD/solid state NMR. RSC Adv 2016;6:103782–90. https://doi.org/10.1039/c6ra17161c.

[48] Clarkson Brian H., Haifeng C. Methods for production and use of synthetic hydroxyapatite and fluorapatite nanorods, and superstructures assembled from the same. US 7,879,388 B2, 2011.

[49] Ferracane JL. Resin-based composite performance: Are there some things we can't predict? Dent Mater 2013;29:51–8. https://doi.org/10.1016/j.dental.2012.06.013.

[50] Heintze SD, Ilie N, Hickel R, Reis A, Loguercio A, Rousson V. Laboratory mechanical parameters of composite resins and their relation to fractures and wear in clinical trials—A systematic review. Dent Mater 2017;33:e101–14. https://doi.org/http://doi.org/10.1016/j.dental.2016.11.013.

[51] Silikas N, Eliades G, Watts DC. Light intensity effects on resin-composite degree of conversion and shrinkage strain. Dent Mater 2000;16:292–6. https://doi.org/http://dx.doi.org/10.1016/S0109-5641(00)00020-8.

[52] Burtscher P. Stability of radicals in cured composite materials. Dent Mater 1993;9:218–21. https://doi.org/10.1016/0109-5641(93)90064-w.

[53] Par M, Gamulin O, Marovic D, Klaric E, Tarle Z. Effect of temperature on post-cure polymerization of bulk-fill composites. J Dent 2014;42:1255–60. https://doi.org/http://dx.doi.org/10.1016/j.jdent.2014.08.004.

[54] Chen YC, Ferracane JL, Prahl SA. Quantum yield of conversion of the photoinitiator camphorquinone. Dent Mater 2007;23:655–64. https://doi.org/10.1016/j.dental.2006.06.005.

[55] Shortall AC, Palin WM, Burtscher P. Refractive index mismatch and monomer reactivity influence composite curing depth. J Dent Res 2008;87:84–8. https://doi.org/10.1177/154405910808700115.

[56] Lovell LG, Stansbury JW, Syrpes DC, Bowman CN. Effects of Composition and Reactivity on the Reaction Kinetics of Dimethacrylate/Dimethacrylate Copolymerizations. Macromolecules 1999;32:3913–21.

https://doi.org/10.1021/ma990258d.

[57] Ilie N, Hilton TJ, Heintze SD, Hickel R, Watts DC, Silikas N, et al. Academy of Dental Materials guidance—Resin composites: Part I—Mechanical properties. Dent Mater 2017;33. https://doi.org/10.1016/j.dental.2017.04.013.

[58] Shah MB, Ferracane JL, Kruzic JJ. R-curve behavior and micromechanisms of fracture in resin based dental restorative composites. J Mech Behav Biomed Mater 2009;2:502–11. https://doi.org/10.1016/j.jmbbm.2008.12.005.

[59] Imbeni V, Kruzic JJ, Marshall GW, Marshall SJ, Ritchie RO. The dentin-enamel junction and the fracture of human teeth. Nat Mater 2005;4:229–32.

[60] Bechtle S, Habelitz S, Klocke A, Fett T, Schneider GA. The fracture behaviour of dental enamel. Biomaterials 2010;31:375–84. https://doi.org/http://doi.org/10.1016/j.biomaterials.2009.09.050.

[61] Bajaj D, Arola DD. On the R-curve behavior of human tooth enamel. Biomaterials 2009;30:4037–46. https://doi.org/http://doi.org/10.1016/j.biomaterials.2009.04.017.

[62] Alshabib A, Silikas N, Watts DC. Hardness and fracture toughness of resin-composite materials with and without fibers. Dent Mater 2019;35:1194–203. https://doi.org/10.1016/j.dental.2019.05.017.

[63] Ilie N, Rencz A, Hickel R. Investigations towards nano-hybrid resin-based composites. Clin Oral Investig 2013;17:185–93. https://doi.org/10.1007/s00784-012-0689-1.

[64] Randolph LD, Palin WM, Leloup G, Leprince JG. Filler characteristics of modern dental resin composites and their influence on physico-mechanical properties. Dent Mater 2016;32:1586–99. https://doi.org/10.1016/j.dental.2016.09.034.

[65] Kim KH, Ong JL, Okuno O. The effect of filler loading and morphology on the mechanical properties of contemporary composites. J Prosthet Dent 2002;87:642–9. https://doi.org/10.1067/mpr.2002.125179.

[66] Aljabo A, Xia W, Liaqat S, Khan MA, Knowles JC, Ashley P, et al. Conversion, shrinkage, water sorption, flexural strength and modulus of re-mineralizing dental composites. Dent Mater 2015;31:1279–89. https://doi.org/http://dx.doi.org/10.1016/j.dental.2015.08.149.

[67] Oral O, Lassila L V., Kumbuloglu O, Vallittu PK. Bioactive glass particulate filler composite: Effect of coupling of fillers and filler loading on some physical properties. Dent Mater 2014;30:570–7. https://doi.org/10.1016/J.DENTAL.2014.02.017.

[68] Jun S-K, Kim D-A, Goo H-J, Lee H-H. Investigation of the correlation between the different mechanical properties of resin composites. Dent Mater J 2013;32:48–57.

[69] Ferracane JL, Berge HX, Condon JR. In vitro aging of dental composites in water - Effect of degree of conversion, filler volume, and filler/matrix coupling. J Biomed Mater Res 1998;42:465–72. https://doi.org/10.1002/(sici)1097-4636(19981205)42:3<465::aid-jbm17>3.0.co;2-f.

[70] Ilie N, Hickel R. Investigations on mechanical behaviour of dental composites.

Clin Oral Investig 2009;13:427. https://doi.org/10.1007/s00784-009-0258-4.

[71] Altaie A, Bubb NL, Franklin P, Dowling AH, Fleming GJP, Wood DJ. An approach to understanding tribological behaviour of dental composites through volumetric wear loss and wear mechanism determination; beyond material ranking. J Dent 2017;59:41–7. https://doi.org/10.1016/j.jdent.2017.02.004.

[72] Mair LH, Stolarski TA, Vowles RW, Lloyd CH. Wear: Mechanisms, manifestations and measurement. Report of a workshop. J Dent 1996;24:141–8. https://doi.org/10.1016/0300-5712(95)00043-7.

[73] Cate JM ten. Current concepts on the theories of the mechanism of action of fluoride. Acta Odontol Scand 1999;57:325–9. https://doi.org/10.1080/000163599428562.

[74] Wiegand A, Buchalla W, Attin T. Review on fluoride-releasing restorative materials--fluoride release and uptake characteristics, antibacterial activity and influence on caries formation. Dent Mater 2007;23:343–62. https://doi.org/10.1016/j.dental.2006.01.022.

[75] Karantakis P, Helvatjoglou-Antoniades M, Theodoridou-Pahini S, Papadogiannis Y. Fluoride release from three glass ionomers, a compomer, and a composite resin in water, artificial saliva, and lactic acid. Oper Dent 2000;25:20–5.

[76] Yap AUJ, Chew CL, Ong L, Teoh SH. Environmental damage and occlusal contact area wear of composite restoratives. J Oral Rehabil 2002;29:87–97. https://doi.org/10.1046/j.1365-2842.2002.00797.x.

[77] McCabe JF, Yan Z, Al Naimi OT, Mahmoud G, Rolland SL. Smart materials in dentistry. Aust Dent J 2011;56:3–10. https://doi.org/10.1111/j.1834-7819.2010.01291.x.

[78] Chan KS, Lee Y-D, Nicolella DP, Furman BR, Wellinghoff S, Rawls R. Improving fracture toughness of dental nanocomposites by interface engineering and micromechanics. Eng Fract Mech 2007;74:1857–71.

[79] Vermeersch G, Leloup G, Vreven J. Fluoride release from glass-ionomer cements, compomers and resin composites. J Oral Rehabil 2001;28:26–32.